ACS APPLIED MATERIALS & INTERFACES

Research Article

www.acsami.org

Luminescent, Freestanding Composite Films of Au_{15} for Specific Metal Ion Sensing

Anu George,[†] E. S. Shibu,[†] Shihabudheen M. Maliyekkal,[†,‡] M. S. Bootharaju,[†] and T. Pradeep*[,†]

[†]DST Unit of Nanoscience (DST UNS), Department of Chemistry, Indian Institute of Technology, Madras, Chennai 600 036, India

[‡]School of Mechanical and Building Sciences, VIT University, Chennai Campus, Chennai-600 048, India

Supporting Information

ABSTRACT: A highly luminescent freestanding film composed of the quantum cluster, Au_{15}, was prepared. We studied the utility of the material for specific metal ion detection. The sensitivity of the red emission of the cluster in the composite to Cu^{2+} has been used to make a freestanding metal ion sensor, similar to pH paper. The luminescence of the film was stable when exposed to several other metal ions such as Hg^{2+}, As^{3+}, and As^{5+}. The composite film exhibited visual sensitivity to Cu^{2+} up to 1 ppm, which is below the permissible limit (1.3 ppm) in drinking water set by the U.S. environmental protection agency (EPA). The specificity of the film for Cu^{2+} sensing may be due to the reduction of Cu^{2+} to Cu^{1+}/Cu^{0} by the glutathione ligand or the Au_{15} core. Extended stability of the luminescence of the film makes it useful for practical applications.

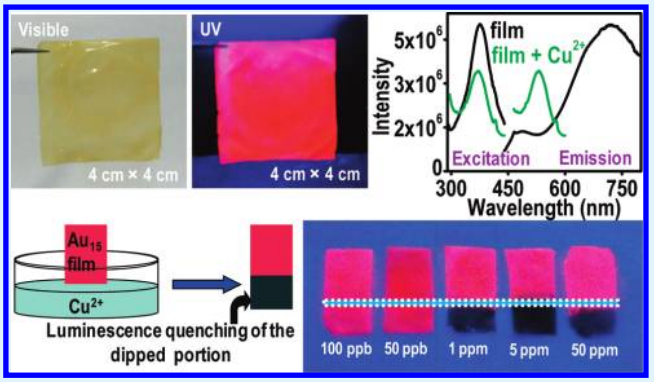

KEYWORDS: *Au_{15} quantum cluster, luminescent films, composite, chitosan, specific metal ion sensing*

INTRODUCTION

Quantum clusters of noble metals are a new category of materials with unusually intense luminescence.[1] Low cytotoxicity, excellent photostability and high quantum yield have made these materials excellent biolabels.[2] Sensitivity of their absorption and luminescence to parameters such as exposed metal ions,[3−5] solvent polarity and hydrogen bonding[2] has been explored in the recent past. Because of the strong quantum size effect, they possess characteristic absorption and emission profiles due to intraband and interband transitions and can be distinguished from the adjacent clusters easily from these features. Metal-enhanced luminescence of such clusters has also been explored.[6] A variety of applications in catalysis,[7,8] electroluminescence,[9] nanoelectronics,[10] soft lithography,[11] bioanalysis,[6,12] etc., are also current excitements in their research.

There are several reports in the recent past on the utilization of gold and silver quantum clusters for Hg^{2+} sensing.[13−16] Metal ion reactivity with luminescent noble metal clusters was pioneered by our group[3] and it has been shown that several Au clusters, especially Au_{23}[2] and Au_{22}[11] are especially selective. No sensitivity was seen for Ag^{+}, Ni^{2+}, Ca^{2+}, Mg^{2+}, Na^{+}, Pb^{2+}, Hg^{2+}, and Cd^{2+} in these clusters.[2] Cu^{2+} is known to be toxic and its allowed level in drinking water is 1.3 ppm, set by the U.S. Environmental Protection Agency (EPA).[17] Creating composite structures using quantum clusters can be directly adapted for applications.[18] These materials are endowed with many important properties such as nonlinear optical properties,[19,20] electronic conductivity[21] and luminescence,[22] and have been suggested for use in various applications including chemical sensors,[23] electroluminescent devices, electrocatalysis,[24] etc.

Although these applications are important, it is necessary to demonstrate the usability of such materials in the device format. For this, it is important to have the materials fabricated in various forms such as films. A free-standing film of a composite may be used for direct applications for metal ions in solution phase, similar to a pH paper. We note that several such nanoscale materials have been prepared in the form of composites for applications of this kind.[25,26] However, no quantum cluster has been developed hitherto in this format adaptable for applications.

One of the newest quantum clusters is Au_{15} encapsulated in cyclodextrin (CD) cavities.[27] While larger clusters are etched by ligands to yield smaller clusters,[28] the product formed is trapped in host cavities to prevent it from further core reduction. Encapsulation allows increased chemical and thermal stability for the cluster. In the present method, Au_{15} cluster protected with glutathione was further stabilized in cyclodextrin cavities. Encapsulation is manifested in 2-dimensional nuclear magnetic resonance (2D NMR) spectroscopy in the form of cross peaks between the protecting glutathione and the encapsulating CD molecules. The size of gold QCs is small

Received: July 2, 2011
Accepted: January 2, 2012
Published: January 2, 2012

to accommodate the cluster inside the CD cavity. The large size of gold nanoparticles limits their incorporation inside the CD cavity. In this work, we present the use of Au_{15} cluster composites for metal ion sensing. A freestanding film of the cluster is shown to be a Cu^{2+} sensor at parts per million concentrations. The luminescence of the film was found to be quenched by Cu^{2+}. Visually detectable changes of the film enable the use of these materials as a Cu^{2+} sensing paper. The extended stable luminescence of the film finds utility in practical applications. Although metal ion sensing in the solution state is known with quantum clusters, specificity to a metal and application as a practical device are demonstrated for the first time.

EXPERIMENTAL SECTION

Materials. All the chemicals were commercially available and used without further purification. $HAuCl_4.3H_2O$, methanol (GR grade), reduced GSH (γ-Glu-Cys-Gly, M.W. = 307), $CuCl_2.2H_2O$, $Cu(OAc)_2{\cdot}H_2O$, $Cu_2Cl_2{\cdot}2H_2O$, and $CuSO_4{\cdot}5H_2O$ were purchased from SRL Chemical Co. Ltd., India. $NaBH_4$ (>90%) was purchased from Sigma Aldrich. β-cyclodextrin (CD) was purchased from Wako Chemicals, Japan. Chitosan was procured from Pelican Biotech & Chemical Laboratories, India.

Synthesis of Au@SG. The nanoparticles protected with −SG ligands (Au@SG) were synthesized using the reported protocol.[27] To a 50 mL methanolic solution (0.5 mM) of $HAuCl_4.3H_2O$, 1.0 mM GSH was added (1:2 molar ratio, total volume of methanol was 50 mL). The mixture was cooled to 0 °C in an ice bath for 30 min. An aqueous solution of $NaBH_4$ (0.2 M, 12.5 mL), cooled to 0 °C, was injected rapidly into the above mixture under vigorous stirring. The mixture was allowed to react for another hour. The resulting precipitate was collected and washed repeatedly with methanol through centrifugal precipitation. Finally the Au@SG precipitate was dried and collected as a dark brown powder. The size of Au@SG particles made here is in the range of 2−3 nm.

Cyclodextrin-Assisted Synthesis of Au_{15} Clusters. The above nanoparticles (50 mg) were dissolved in 40 mL of deionized (DI) water containing 1.6 mol of GSH and 2.2×10^{-4} mol of cyclodextrin. In this synthesis, GSH is used in excess as it works as an etchant. The mixture was heated at 70 °C for 48 h. The completion of the reaction was monitored by checking the red emission of the cluster under UV light. The entire solution was centrifuged at 5000 rpm for 10 min. The supernatant was transferred to a plastic vial and solution was freeze-dried to obtain a brown powder with intense red emission in the solid state. The material was washed twice with ethanol to remove excess GSH.

Preparation of Cluster Composite Film. Two grams of chitosan is dissolved with stirring in 50 mL of distilled water containing 5% glacial acetic acid. Insoluble substances are removed by filtration through a medium-pore-sized glass funnel to yield chitosan solution. Twenty milliliters of chitosan solution is poured onto plastic petridish and dried at 40 °C for 24 h. The film so obtained is soaked in 20 mL solution of 5% trisodium citrate to enhance the strength and was washed thoroughly and dried. A free-standing film of Au_{15} incorporated chitosan was prepared by soaking the film in Au_{15} cluster solution for 10 min and dried. Uptake of Au_{15} was manifested in the form of bright luminescence of the film upon UV irradiation.

Methods. Ultraviolet−visible (UV−vis) spectra were recorded using a PerkinElmer Lambda 25 spectrophotometer. The photo-excitation and luminescence (PL) studies were done using a NanoLog HORIBA JOBINYVON spectrofluorimeter. Band pass for both excitation and emission monochromators was kept at 3 nm. Scanning electron microscopic (SEM) images and energy-dispersive analysis of X-rays (EDAX) studies were obtained using a FEI QUANTA-200 SEM. Attenuated total reflection infrared spectroscopy (ATR−IR) was measured using PerkinElmer Spectrum 100 Spectrometer. Chlorides (Cu^{2+}, Cu^{1+}, and Hg^{2+}), sulfates, acetates (Cu^{2+}), arsenates, and arsenites (Na^+) were used for metal ion detection studies. Metal ion detection was studied at ppm concentrations. X-ray photoelectron spectroscopy measurements were conducted using an Omicron ESCA Probe spectrometer with unmonochromatized Al Kα X-rays (energy = 1486.6 eV).

RESULTS AND DISCUSSION

Au_{15} shows a well-defined optical absorption spectrum in aqueous solution with features at 318, 458, and 580 nm, all of which are marked in Figure 1. The absorption features of

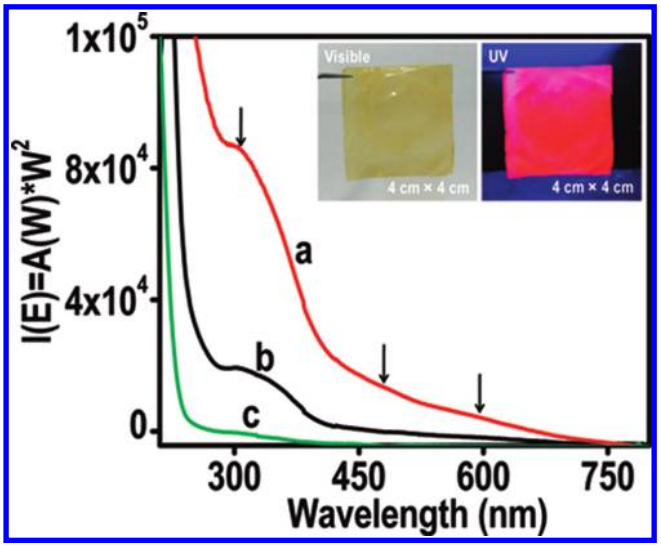

Figure 1. Time-dependent UV/vis spectra of Au_{15} cluster solution in which the parent film was soaked. Traces a, b, and c correspond to 2, 6, and 10 min of exposure, respectively. Inset shows the photographs of the cluster incorporated film under white light and UV light.

Au_{15}@CD are not sharp, unlike in the case of QCs such as Au_{25},[29] Au_{22},[11] and Au_{23}.[2] Optical luminescence, solvent dependency, metal ion sensing, gelation are some of the reported properties of Au_{15}.[27] Upon exposing a freestanding film of chitosan to the Au_{15} solution, the cluster gets loaded onto the film. The spectra of the solution after various intervals of exposure of the chitosan film are shown in Figure 1. The decrease in the intensity of the peaks shows that the cluster is getting loaded onto the film. The film after loading the cluster shows luminescence as shown in the inset of Figure 1. A time-dependent color change of the Au_{15} solution is observed during loading. Initially the solution shows high luminescence on UV irradiation, which gradually disappears with respect to time.

A saturation uptake of the cluster was observed after ten minutes of exposure as shown in Figure 2. From the decrease in intensity of optical absorption of Au_{15}, a maximum uptake of 0.06×10^{-4} mol per sq. cm can be inferred. Beyond this, no further uptake happens as shown by the inset of Figure 2. Uptake of Au_{15} is manifested in the form of bright luminescence of film upon UV irradiation (inset of Figure 1).

The morphology of the film was studied using SEM. A higher-magnification image of an edge of the composite film is shown in Figure 3. To study the spatial distribution of gold and sulfur in the film formed by QCs, we carried out elemental mapping using EDAX. Figure 3A shows the EDAX spectrum collected from the film. Elemental maps are given as inset a_1 and a_2 in Figure 3A. The data confirm the uniform presence of the cluster in the composite. Luminescence of the parent chitosan film appears at 500 nm, far away from the cluster emission (in the Supporting Information, discussed later). The

dx.doi.org/10.1021/am201292a | ACS Appl. Mater. Interfaces 2012, 4, 639−644

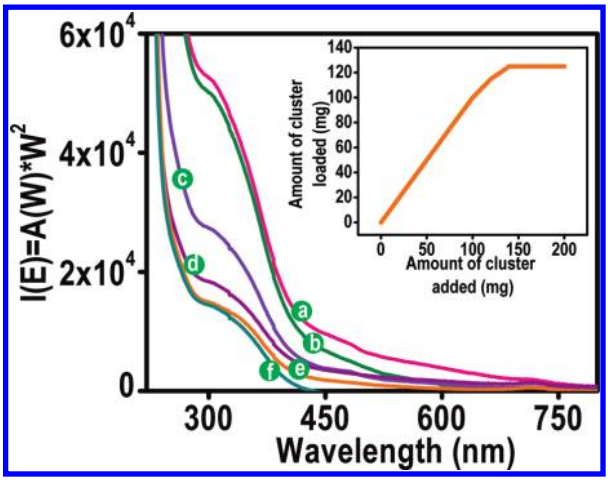

Figure 2. Time-dependent UV/vis spectra of Au_{15} cluster solution at the saturation point. Traces a–f correspond to 0, 2, 4, 6, 8, and 10 min of exposure, respectively. Inset shows the saturation uptake of the cluster after 10 min of soaking.

photoluminescence spectrum of the Au_{15} cluster (in solution form) used in the study is given in the Supporting Information (Figure S1). The luminescence spectrum of the composite film is shown in Figure 3. The spectrum is comparable to that of Au_{15} in the solution phase, which shows a similar bright red luminescence on UV irradiation. Au_{15} shows a NIR emission with a maximum of 690 nm for excitation at 375 nm. PL spectra of these quantum clusters show a large stokes shift. Possible reason for this could be the energy cascade within the sp derived excited states, facilitated by the concomitant energy relaxation through structural distortion and low energy excitation of the ligands. The composite film, when excited around 375 nm, shows an emission around 700 nm which resembles that of the Au_{15} solution. This confirms the molecular nature of the cluster in the composite film. Corresponding photographs of Au_{15} and the composite film under the UV light are shown as the inset of Figure 3B.

Attenuated total reflection infrared spectroscopy (ATR–IR) was employed to investigate the chemical affinity of Au_{15} to the surface of the film. Figure 4 shows the ATR–IR spectra of the

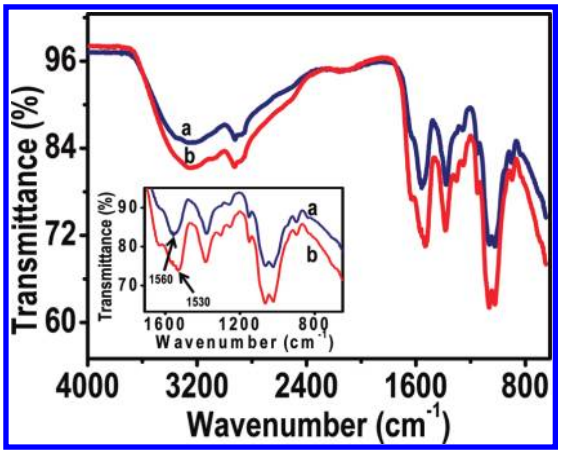

Figure 4. ATR–IR spectra of the parent film (trace a) and the composite (trace b). Inset shows an expanded view of the fingerprint region of the composite.

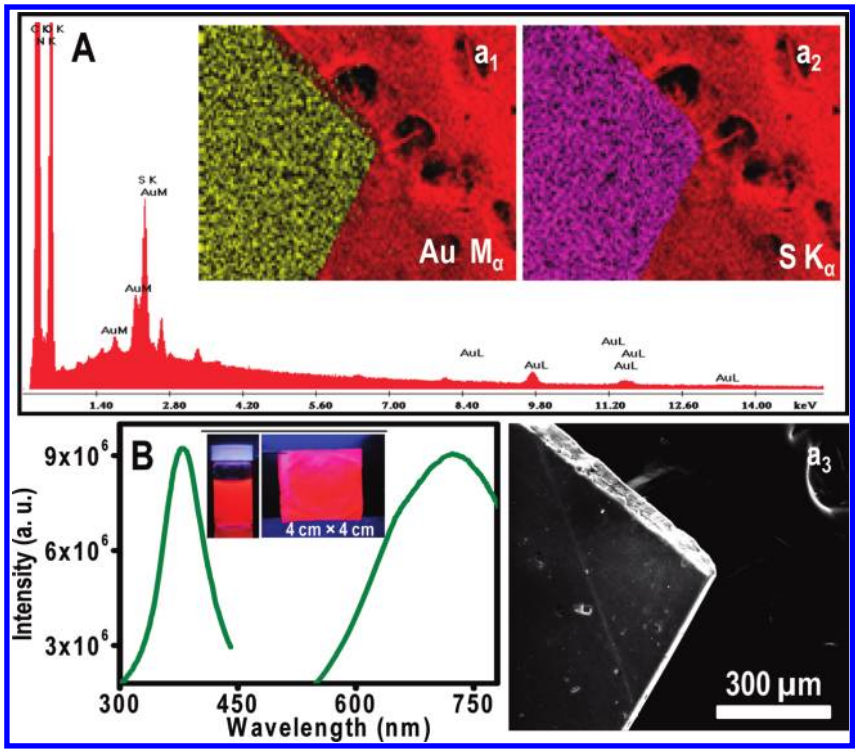

Figure 3. (A) EDAX spectrum of the composite film formed by the quantum cluster. (a_1), (a_2) EDAX mapping of the film using Au M_α and S K_α lines, respectively. The corresponding SEM image in a_3. The uniform red background in a_1 and a_2 is due to the conducting carbon tape on which the composite film was placed. (B) PL spectrum of cluster-chitosan film. Peaks in UV and visible regions correspond to excitation and emission, respectively. Inset of B shows the photographs of aqueous Au_{15} solution and the film under the UV light.

dx.doi.org/10.1021/am201292a | ACS Appl. Mater. Interfaces 2012, 4, 639–644

parent chitosan film (trace a) and the composite (trace b). The characteristic absorption bands of chitosan are the bands at 1560 cm^{-1}, due to the stretching vibration of the amino group, and that at 1334 cm^{-1}, assigned to the C−H stretching vibration. Another band around 3336 cm^{-1} is due to the amine N−H symmetric vibration. The peak at 2927 cm^{-1} is the typical C−H stretching vibration. The peaks around 897 and 1154 cm^{-1} correspond to the saccharide structure of chitosan. The broad peak at 1081 cm^{-1} is due to the C−O stretching vibration. A comparison with the chitosan film shows that the band at 1560 cm^{-1} corresponding to the amino group stretching is shifted in the composite (trace b). All the other features are essentially unaltered. Therefore, we suggest that the binding of the Au_{15} to the film occurs due to the interaction of amino group (NH_3^+) on chitosan with COO^- functionalities on the cluster.

The transmittance spectra of the parent chitosan film and the cluster incorporated film were analyzed and shown in Figure 5.

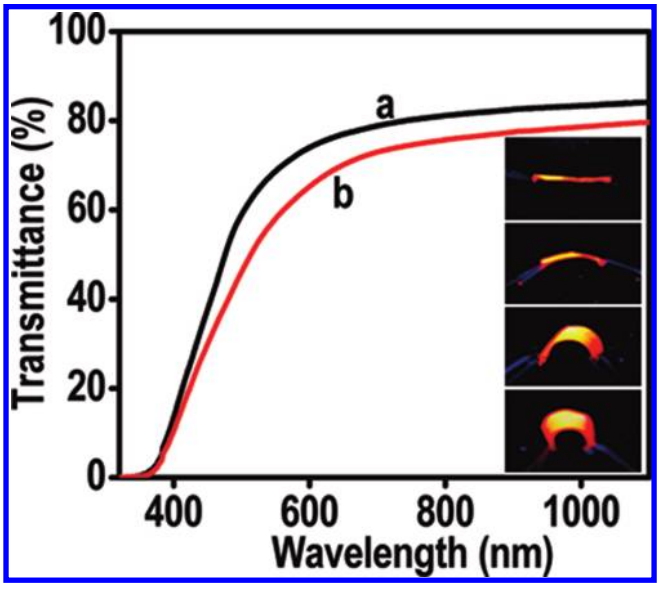

Figure 5. Transmittance of parent chitosan film (trace a) and the composite (trace b) as a function of wavelength ranging from 300 to 1100 nm. Inset shows the photographs of the composite film under UV light upon bending.

A transmittance of 80% is observed in the case of the parent film (trace a). After the loading of the cluster, the transmittance was reduced by 10% (trace b). Appreciable optical transparency to visible and near-infrared light promises its utility in making transparent, luminescent films with applications, ranging from flat panel displays to photovoltaic cells. The film is flexible and the luminescence is retained. Photographs of the film under the UV light at different extent of bending are shown in Figure 5.

The red emission from the cluster was utilized for selective metal ion detection. In the case of parent Au_{15} in solution, we could see a drastic change, such as immediate disappearance of red emission followed by the emergence of yellow emission when exposed to Cu^{2+}, and no effect was observed for several other metal ions tested.[27] However, the film incorporated with Au_{15} shows specific sensing for Cu^{2+} by immediate quenching of the luminescence. The detection studies were carried out at ppm concentrations. A drastic change in the emission maximum was seen in the PL spectra of the film before and after exposure of Cu^{2+} (Figure 6A, traces a and b, respectively). The quenching of luminescence in the case of Cu^{2+} is abrupt. This exposure to Cu^{2+} makes an irreversible colored stain on the film. The parent chitosan film shows a decrease in luminescence intensity and a blue shift of 7 nm in peak maximum upon exposure to 5 ppm Cu^{2+} (see Figure S2 in the Supporting Information). The composite film was exposed to several other metal ions as well (Figure 6B). Although there is a decrease in luminescence upon exposure to Hg^{2+}, As^{5+} and As^{3+} (Figure 6B, traces b, c and d, respectively), the luminescence recovers upon drying the film, unlike in the case of Cu^{2+}. A film upon exposure to pure water itself shows a decrease in luminescence, but it recovers upon drying. Thus the decrease obtained with other metal ions is due to the solvent. Traces labeled a in Figures 6A and B are due to the composite film alone.

A prototypical sensor film was fabricated which shows the effectiveness of the material. Figure 6C shows photographs of the films exposed to various concentrations of Cu^{2+}. The concentration of Cu^{2+} was varied from 50 ppb to 50 ppm. The region exposed to Cu^{2+} shows visible color change and the intensity of the color is proportional to Cu^{2+} concentration. The exposed film is stable for an extended period; the parent composite film is also stable for a long time. EDAX analysis showed that the Cu^{2+} exposed film showed uniform

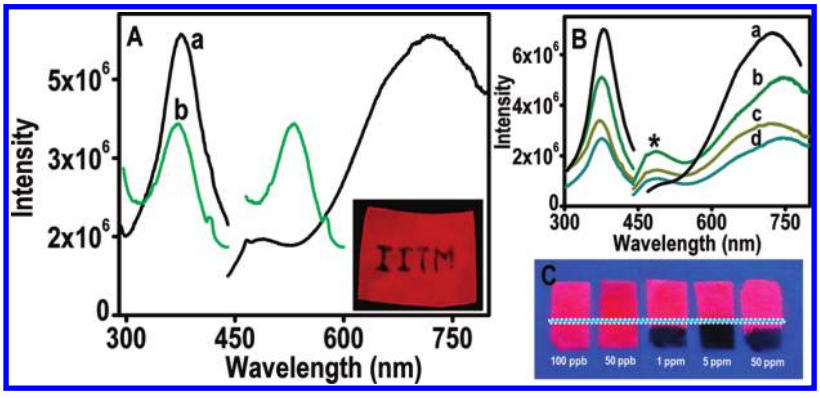

Figure 6. (A) PL spectra of the film before and after exposing to Cu^{2+} (traces a and b, respectively). Inset shows the pattern written on the film using Cu^{2+} in solution. (B) PL spectra of the film exposed to Hg^{2+}, As^{5+} and As^{3+} (traces b, c and d, respectively). Trace a is due to composite film alone. Peaks in UV and visible regions correspond to excitation and emission, respectively (both in A and B). (C) Dependence of Cu^{2+} concentration on luminescence quenching. Peaks marked with an asterisk (*) in B correspond to the emission of chitosan.

concentration of Au, Cu, S and Cl (see Figure S3 in the Supporting Information).

To understand the specificity to Cu^{2+} and also the negligible response to Hg^{2+}, we performed XPS studies. The cluster in the solution phase was treated with metal ions such as Cu^{2+} and Hg^{2+} for 10 min such that their final concentration was 5 ppm. The samples were freeze-dried and washed with methanol in order to remove the possibility of physical adsorption. The precipitate collected on washing was spotted on a molybdenum sample plate and dried in vacuum. The spectra in the required binding energy (BE) range were collected. Figure 7A shows the

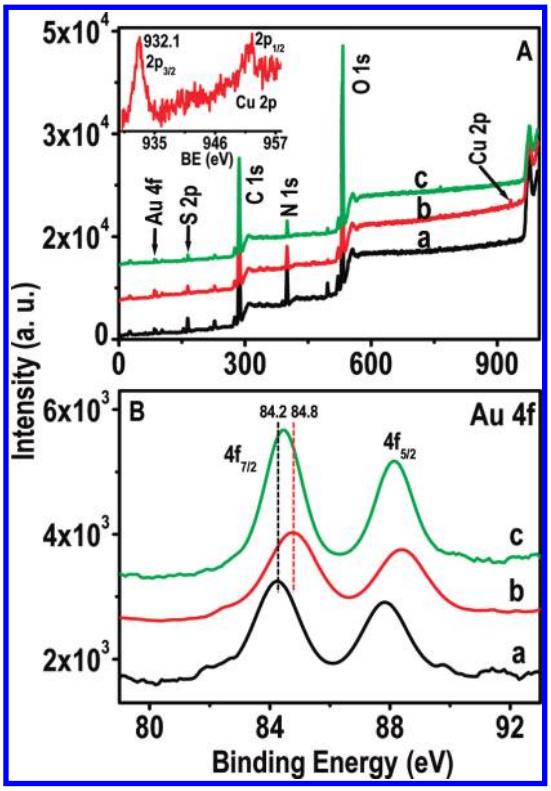

Figure 7. A and B are survey spectra and Au 4f regions, respectively of a) Au_{15}@SG-βCD, b) Au_{15}@SG-βCD+Cu^{2+} and c) Au_{15}@SG-βCD +Hg^{2+}. Inset of A is Cu 2p region of sample b. The dotted lines in B indicate the change in BE. Minor shift in c (0.2 eV) is within the variations seen typically.

XPS survey spectra of Au_{15}@SG-βCD, Au_{15}@SG-βCD+Cu^{2+} and Au_{15}@SG-βCD+Hg^{2+} (traces a, b and c, respectively) and the detailed spectra are collected at a pass energy of 20 eV for specific regions (7B and inset of 7A). The presence of gold, sulfur, carbon, nitrogen, oxygen and copper is evident from the survey spectra. The Au $4f_{7/2}$ for both Au_{15}@SG-βCD and Au_{15}@SG-βCD+Hg^{2+} (Figure 7B, traces a and c, respectively) appear at 84.2 (±0.2) eV, corresponding to the characteristic binding energy of gold in zerovalent state.[30] The Au $4f_{7/2}$ feature of copper treated sample is shifted by a significant value (+0.6 eV, Figure 7B, trace b) which shows the interaction of the cluster with copper. This supports the change in the luminescence of Au_{15}@SG-βCD. The Cu 2p region of Au_{15}@SG-βCD+Cu^{2+} is shown as inset of Figure 7A. This shows a feature of Cu $2p_{3/2}$ at 932.1 eV with the absence of satellite. The absence of satellite indicates the absence of copper in the +2 state.[31] The peak at 932.1 eV may be due to Cu^{1+} or Cu^0 as their binding energies are very close (by only 0.1−0.2 eV) and differentiation is difficult by XPS.[31] The reduction of Cu^{2+} to Cu^{1+}/Cu^0 may be due to the interaction of glutathione ligands of the cluster as glutathione is well-known to reduce Cu^{2+} to Cu^{1+}.[32] The other possibility is the reduction of Cu^{2+} by Au_{15} core where redox reaction may be feasible at the size scale of quantum clusters. This change is expected to affect the luminescence greatly. The Hg 4f region of Au_{15}@SG-βCD +Hg^{2+} is shown in Figure S4 in the Supporting Information. Mercury is not detected. This may be due to negligible/weak interactions of Hg^{2+} with glutathione ligands of the cluster. The feature observed in this binding energy region is due to Au 5s.

The sensitivity of the composite film to various salts of Cu^{2+} was also checked. All the salts of Cu^{2+} (such as chloride, sulfate and acetate) showed a similar shift in the emission wavelength (see Figure S5 in the Supporting Information). The sensitivity to Cu^{1+} in ppm concentration was also investigated which showed a shift similar to Cu^{2+} but larger in magnitude (see Figure S6 in the Supporting Information). Dependence of the emission features on the anions and valence state of copper are subtle at the concentrations tested but they suggest that these aspects are also significant.

CONCLUSION

A multifunctional freestanding film of cm^2 area composed of Au_{15} cluster was fabricated. We demonstrated the utility of the film as a practical metal ion sensor. The visually observable changes are proportional to the metal ion concentration. The sensitivity of the luminescence to various cations was investigated in which the material showed an abrupt change in the case of Cu^{2+} and there is no effect when several other ions were tested. The stability of the composite, sensitivity to lower concentration, applicability across all anions and absence of other metal ion induced changes make this system useful for practical applications. The specific sensing of Cu^{2+} is understood by XPS analysis which reveals the reduction of Cu^{2+} to Cu^{1+}/Cu^0 either by the glutathione ligand or the Au_{15} core.

ASSOCIATED CONTENT

Supporting Information

Excitation/emission spectrum and photograph of Au_{15} in solution phase under visible light, photoluminescence spectra of chitosan film with and without Cu^{2+}, EDAX spectrum and SEM/EDAX image of the film in the presence of Cu^{2+}, XPS of Au_{15}@SG-βCD+Hg^{2+} sample in the Hg 4f region, PL spectra of the composite film on exposure to different compounds of Cu^{2+} and comparison of the emission spectra of the film with Cu^{1+} and Cu^{2+}. This material is available free of charge via the Internet at http://pubs.acs.org.

AUTHOR INFORMATION

Corresponding Author

*E-mail: pradeep@iitm.ac.in.

ACKNOWLEDGMENTS

We thank Department of Science and Technology, Government of India for constantly supporting our research program on nanomaterials.

REFERENCES

(1) Muhammed, M. A. H.; Pradeep, T In *Advanced Fluorescence Reporters in Chemistry and Biology II*; Demchenko, A. P, Ed.; Springer-Verlag: Berlin, 2010; Vol. 9, part 4, pp 333−353.

(2) Muhammed, M. A. H.; Verma, P. K.; Pal, S. K.; Kumar, R. C. A.; Paul, S.; Omkumar, R. V.; Pradeep, T. *Chem.—Eur. J.* **2009**, *15*, 10110−10120.
(3) Muhammed, M. A. H.; Pradeep, T. *Chem. Phys. Lett.* **2007**, *449*, 186−190.
(4) Shichibu, Y.; Negishi, Y.; Tsunoyama, H.; Kanehara, M.; Teranishi, T.; Tsukuda, T. *Small* **2007**, *3*, 835−839.
(5) Adhikari, B.; Banerjee, A. *Chem. Mater.* **2010**, *22*, 4364−4371.
(6) Muhammed, M. A. H.; Verma, P. K.; Pal, S. K.; Retnakumari, A.; Koyakutty, M.; Nair, S.; Pradeep, T. *Chem.—Eur. J.* **2010**, *16*, 10103−10102.
(7) Tsunoyama, H.; Sakurai, H.; Ichikuni, N.; Negishi, Y.; Tsukuda, T. *Langmuir* **2004**, *20*, 11293−11296.
(8) Tsunoyama, H.; Sakurai, H.; Negishi, Y.; Tsukuda, T. *J. Am. Chem. Soc.* **2005**, *127*, 9374−9375.
(9) Gonzalez, J. I.; Lee, T. H.; Barnes, M. D.; Antoku, Y.; Dickson, R. M. *Phys. Rev. Lett.* **2004**, *93*, 147402−147405.
(10) Chen, S.; Ingram, R. S.; Hostetler, M. J.; Pietron, J. J.; Murray, R. W.; Schaaff, T. G.; Khoury, J. T.; Alvarez, M. M.; Whetten, R. L. *Science* **1998**, *280*, 2098−2101.
(11) Shibu, E. S.; Radha, B.; Verma, P. K.; Bhyrappa, P.; Kulkarni, G. U.; Pal, S. K.; Pradeep., T. *ACS Appl. Mater. Interfaces* **2009**, *1*, 2199−2210.
(12) Cui, Y.; Ren, B.; Jao, J. L.; Gu, R. A.; Tian, Z. Q. *J. Phys. Chem. B* **2006**, *110*, 4002−4006.
(13) Lin, Y. H.; Tseng, W. L. *Anal. Chem.* **2010**, *82*, 9194−9200.
(14) Wei, H.; Wang, Z.; Yang, L.; Tian, S.; Hou, C.; Lu, Y. *Analyst* **2010**, *135*, 1406−1410.
(15) Xie, J.; Zheng, Y.; Ying, J. Y. *Chem. Commun.* **2010**, *46*, 961−963.
(16) Bootharaju, M. S.; Pradeep, T. *Langmuir* **2011**, *27*, 8134−8143.
(17) Su, Y. T.; Lan, G. Y.; Chen, W. Y.; Chang, H. T. *Anal. Chem.* **2010**, *82*, 8566−8572.
(18) Sreeprasad, T. S.; Maliyekkal, S. M.; Krishnan, D.; Chaudhari, K.; Xavier, P. L.; Pradeep, T. *ACS Appl. Mater. Interfaces* **2011**, *3*, 2643−2654.
(19) Irimpan, L.; Nampoori, V. P. N; Radhakrishnan, P. *J. Appl. Phys.* **2008**, *103*, 094914 (1−8).
(20) Srivastava, S.; Haridas, M.; Basu, J. K. *Bull. Mater. Sci.* **2008**, *31*, 213−217.
(21) Gelves, G. A.; Mohammed, H.; Salehab, A.; Sundararaj, U. *J. Mater. Chem.* **2011**, *21*, 829−836.
(22) Zhou, H.; Chen, X.; Wu, G.; Gao, F.; Qin, N.; Bao, D. J. *Am. Chem. Soc.* **2010**, *132*, 1790−1791.
(23) Bubb, D. M.; McGill, R. A.; Horwitz, J. S.; Fitz-Gerald, J. M.; Houser, E. J.; Stroud, R. M.; Wu, P. W.; Ringeisen, B. R.; Pique, A.; Chrisey, D. B. *J. Appl. Phys.* **2001**, *89*, 5739−5746.
(24) Zhou, Q.; Li, C. M.; Li, J.; Cui, X.; Gervasio, D. *J. Phys. Chem. C* **2007**, *111*, 11216−11222.
(25) Liu, X.; Hu, Q.; Fang, Z.; Zhang, X.; Zhang, B. *Langmuir* **2009**, *25*, 3−8.
(26) Kampalanonwat, P.; Supaphol, P. *ACS Appl. Mater. Interfaces* **2010**, *2*, 3619−3627.
(27) Shibu, E. S.; Pradeep, T. *Chem. Mater.* **2011**, *23*, 989−999.
(28) Shibu, E. S.; Muhammed, M. A. H.; Tsukuda, T.; Pradeep, T. *J. Phys. Chem. C* **2008**, *112*, 12168−12176.
(29) Zhu, M.; Lanni, E.; Garg, N.; Bier, M. E.; Jin, R. *J. Am. Chem. Soc.* **2008**, *130*, 1138−1139.
(30) Negishi, Y.; Nobusada, K.; Tsukuda, T. *J. Am. Chem. Soc.* **2005**, *127*, 5261−5270.
(31) Ai, Z.; Zhang, L.; Lee, S.; Ho, W. *J. Phys. Chem. C* **2009**, *113*, 20896−20902.
(32) Anwar, Z. M. *J. Chin. Chem. Soc.* **2005**, *52*, 863−871.